Polarization Characteristics of Scattered Radiation from a Diffraction Grating by Ellipsometry with Application to Surface Roughness*

R. M. A. Azzam and N. M. Bashara
Electrical Materials Laboratory† and Electrical Engineering Department, The University of Nebraska, Lincoln, Nebraska 68508
(Received 15 October 1971)

The polarization properties of the various diffracted orders from a grating are determined ellipsometrically. The ratio ρ_m of the far-field complex reflection coefficients for the p and s polarizations for any order m is measured. This information is complementary to the data available from the partition of the scattered energy over the radiating orders. By examining the polarization of the specularly reflected zeroth-order beam at large angles of incidence the optical effect of surface roughness is established. The roughened surface layer is shown to be equivalent to a film whose index of refraction is the average of the indices of the material of the surface and the immersion medium, in accordance with the Maxwell Garnett theory. The film thickness is a measure of the surface roughness. To explain the ellipsometric results on the various orders we derived an expression for ρ_m starting from the Stratton-Silver-Chu integral using the physical-optics approximation. There is agreement between the gross features of the theory and experiment, but the exact magnitudes could not be compared. This points to the need for an exact solution of the grating-diffraction problem for both polarizations, including the effect of a finite conductivity at optical frequencies.

I. INTRODUCTION

Diffraction gratings have been the subject of continued interest both theoretical and experimental.[1] These devices find their most useful application in spectrometers and have distinct advantages as coupling mirrors in the resonators of lasers and masers.[2,3]

In surface studies, the diffraction of a laser beam by a specially prepared gratinglike corrugated surface profile is used to study surface self-diffusion.[4] Annealing the surface smooths out the corrugations, and from the kinetics of this process atomic mobilities on the surface are readily obtained. Grating diffraction also serves as a means of studying surface plasmons and their dispersion.[5]

In this paper we direct attention to the importance of using ellipsometry to measure the polarization characteristics of the various diffracted orders from a grating. This technique is capable of measuring the ratio ρ_m of the complex reflection coefficients of the p and s polarizations, respectively, for any diffracted order m. These coefficients involve the far fields along the incident beam and any diffracted order. The coefficients are different from local or near-field reflection coefficients of the Fresnel type. For a given grating at a particular wavelength and angle of incidence, the set of complex numbers ρ_m ($m = 0, \pm 1, \pm 2, \ldots$) determines the polarization of the various reflected orders for any incident polarization form. Previously, the emphasis in the analysis of diffraction gratings has been on the distribution of the scattered energy over the various orders of diffraction. Ellipsometry, being a polarization-sensitive technique, offers the means of obtaining complementary information on polarization alone. It is expected that ρ_m, besides its dependence on the detailed groove shape, would be a very sensitive function of the complex optical dielectric constants of the materials forming the grating surface. For example, ellipsometer measurements on an $Al + MgF_2$ grating surface cannot be explained if the presence of the magnesium-fluoride layer on top of the aluminum is neglected. Although a number of exact boundary-value-problem techniques have been developed recently for the grating problem,[6-11] they either have been limited to one polarization or assume infinite conductivity. For ellipsometric measurements, the incident light must necessarily have components of both p and s polarizations and the assumption of perfect conductivity cannot be made. In this paper we compare our experimental results with those predicted by the physical-optics approximation. The kind of agreement obtained is discussed.

Important conclusions can be reached on the optical effect of the ruled surface by examining the polarization of the zeroth-order diffracted beam at large angles of incidence. The grating surface is found to be equivalent to a filmed substrate and the interpretation of the parameters of this optical model is discussed. Since the grating is an example of a deterministically rough surface, this result provides a useful interpretation of the effect of surface roughness, a problem of great interest in optics.

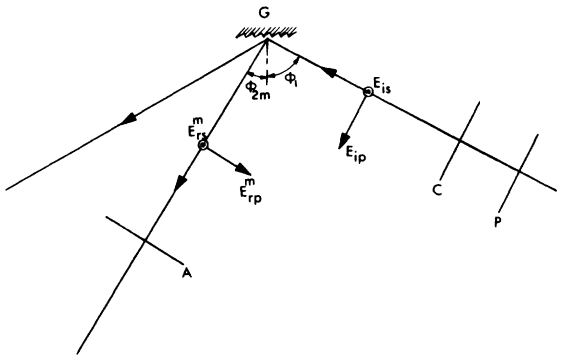

FIG. 1. Ellipsometer arrangement for measuring the ratio ρ_m of the far-field complex reflection coefficients for the p and s polarizations for any diffracted order m, Eqs. (1)–(3). With the compensator C set at a fixed azimuth, the polarizer P and the analyzer A are adjusted to minimize the light flux from the mth-order diffracted beam falling on the photodetector. ϕ_1 and ϕ_{2m} are the angle of incidence and the angle of diffraction of the mth order, respectively.

Section II gives basic definitions and description of the measurement technique. In Sec. III the experimental results on a 1200-lines/mm grating are presented. The interpretation of the polarization of the zeroth-order diffracted beam on the basis of a filmed-substrate model is found in Sec. IV. The agreement between the experimental results and the predictions of the physical-optics approximation is discussed in Sec. V. Section VI summarizes the important conclusions of this paper.

II. DEFINITIONS AND DESCRIPTION OF MEASUREMENT PROCEDURE

The diffraction grating is mounted on the specimen table of the ellipsometer and is aligned so that the reflected zeroth-order (specular) beam passes through the analyzer telescope at the desired angle of incidence. The direction of the grooves is adjusted perpendicular to the plane of incidence which is formed by the incident and the specularly reflected zeroth-order beams. This is effected by rotating the grating surface around its normal until all the diffracted orders lie in that plane. Under this condition, a simple rotation of the analyzer arm allows any of the orders to pass through the analyzer telescope, which has two pinholes at its ends.

Figure 1 shows a schematic of the arrangement of the optical components of the ellipsometer. P, C, G, and A represent the polarizer, compensator, grating surface, and analyzer, respectively. The analyzer arm is rotated to sample the various orders of the scattered radiation. With the compensator set at azimuth $C = 45°$, the light flux from the mth order falling on the photodetector is minimized by adjustment of the polarizer and analyzer. These nulling angles determine the change in the state of polarization between the incident and mth-order beams. Using the notation of conventional ellipsometry, the quantity

$$\rho_m = \tan\psi_m e^{i\Delta_m} \tag{1}$$

can be determined. Let E_{ip} and E_{is} denote the complex amplitudes of the components of the electric vector of the incident light beam parallel and perpendicular to the plane of incidence, respectively, and E^m_{rp} and E^m_{rs} denote the same quantities for the mth-order reflected beam. These fields are taken at points on the respective beams which are very far (in terms of wavelengths) removed from the grating surface. Then

$$\rho_m = R^m_p / R^m_s \quad , \tag{2}$$

where

$$R^m_p = E^m_{rp}/E_{ip}, \quad R^m_s = E^m_{rs}/E_{is} \quad . \tag{3}$$

R^m_p and R^m_s are complex reflection coefficients that relate the components of the far-field electric vector of the incident and mth-order diffracted beams. In this respect they are different from the usual Fresnel reflection coefficients of a perfectly smooth surface which apply to the fields in the immediate vicinity of the surface. Obviously, the ellipsometer senses the far fields only and not the near fields right on the grating surface.

The physical meaning of the complex quantities ρ_m ($m = 0, \pm 1, \pm 2, \ldots$) becomes clear if we consider the diffraction of linearly polarized incident light whose azimuth is 45° from the plane of incidence. In this case $1/\rho_m$ gives the complex-number representation of the elliptic polarization state of the mth diffracted order. The azimuth θ (measured from the plane of incidence) and ellipticity $\tan\epsilon$ of the corresponding vibration ellipse are determined by

$$\frac{1}{\rho_m} = \frac{\tan\theta + i\tan\epsilon}{1 - i\tan\theta\tan\epsilon} \quad . \tag{4}$$

In the general case of incident light in polarization state χ_i, the mth diffracted order has a polarization state χ_i/ρ_m. Details regarding the representation of polarization states by complex numbers and its consequences can be found elsewhere.[12]

The relation between the instrument readings (i.e., the polarizer-analyzer azimuth-angle pair at null) and ψ_m and Δ_m taking into account the real behavior of the optical components of the ellipsometer has been studied extensively by the authors.[13]

III. EXPERIMENTAL RESULTS

The measurements reported here were made at

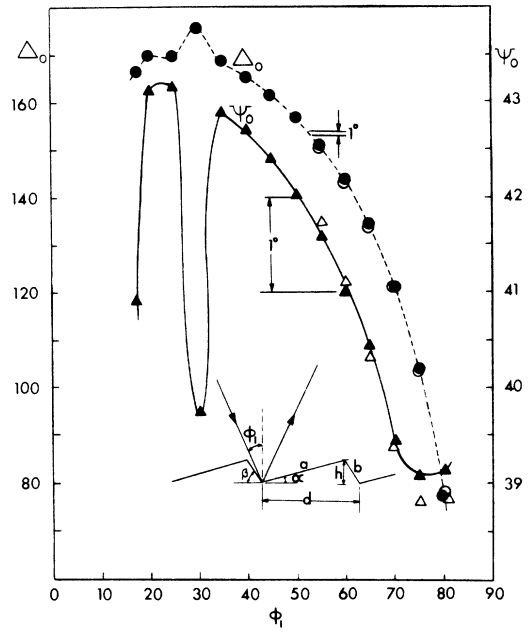

FIG. 2. Variation with angle of incidence (ϕ_1) of the ellipsometric parameters ψ_0(▼) and Δ_0(●) of the zeroth-order beam diffracted by a 1200-lines/mm Al-coated echelette grating at $\lambda = 6328$ Å. The insert shows the geometry of the echelette grating where $d = 8333.3$ Å, $\alpha = 10.3°$, and $\beta = 60°$. The open circles (○) and triangles (▽) correspond to values computed on the basis of a filmed-substrate model for the grating surface. ϕ_1, Δ_0, and ψ_0 are in degrees.

6328 Å on an aluminum-coated 1200-lines/mm echelette diffraction grating with groove sides inclined at 10.3° and 60° from the mean surface level (MSL).[14] The ellipsometer nulling angles in two zones were obtained for the zeroth-, first-, and second-order beams over a range of angle of incidence from 17.5° to 80°. The first-order beam was accessible over the range 40°–80°, and for the second order the accessibility was limited to the 70°–80° range. The limitation was simply due to the fact that the angle between the two arms of the ellipsometer could not be made less than 35°.

The directions of the diffracted orders as measured were found to be in good agreement with those predicted by the grating equation

$$\sin\phi_{2m} = \sin\phi_1 - m\lambda/d, \quad m = 0, 1, 2, \ldots , \qquad (5)$$

where ϕ_1 and ϕ_{2m} represent the angle of incidence and the angle of diffraction of the mth order, respectively, as shown in Fig. 1. $\lambda = 6328$ Å is the wavelength of the incident laser beam and $d = 8333.3$ Å is the interline spacing of the grating. For the range of ϕ_1 indicated above, only positive values of m are allowed by Eq. (5) and all diffracted orders were on one side of the specular zeroth-order beam towards the normal to the MSL.

The variation with angle of incidence of the ellipsometric parameters ψ_0 and Δ_0 of the zeroth-order beam is shown in Fig. 2. Note the expanded scale of ψ_0 as compared to that of Δ_0. The values of ψ_0 and Δ_0 vary within the ranges $39.06° \leq \psi_0 \leq 43.17°$ and $77.39° \leq \Delta_0 \leq 175.64°$, respectively, when ϕ_1 is changed from 17.5° to 80°. Therefore, when the incident light is linearly polarized at azimuth 45° from the plane of incidence, the p and s components of the electric vector of the zeroth-order beam maintain nearly equal amplitudes (within ~20%, with the s component always larger), whereas their relative phase Δ_0 changes by as much as ~100° owing to the change in angle of incidence. Clearly, a distinguished feature in Fig. 2 is the anomalous dip and peak in the curves of ψ_0 and Δ_0, respectively, at $\phi_1 = 30°$.

Figure 3 gives the data for (ψ_1, Δ_1) and (ψ_2, Δ_2). Although Δ_1 and Δ_2 exhibit a dependence on ϕ_1 similar to that of Δ_0, ψ_1 and ψ_2 increase with the increase of ϕ_1, whereas ψ_0 decreases for large values of ϕ_1. Thus the higher diffracted orders

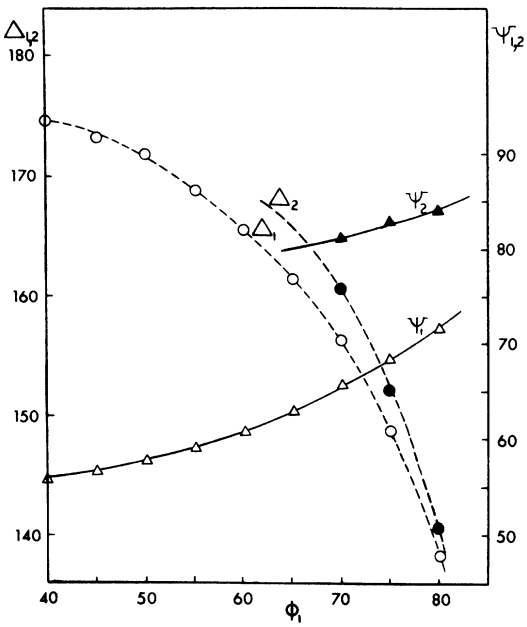

FIG. 3. Variation of the ellipsometric parameters (ψ_1, Δ_1) and (ψ_2, Δ_2) on the first- and second-order beams, respectively, with the angle of incidence ϕ_1 for the same grating as in Fig. 2. The results of both Figs. 2 and 3 refer to off-blaze measurements. The on-blaze measurements (obtained after a 180° rotation of the grating) show similar behavior with angle of incidence. The magnitudes of ψ_0 and Δ_0 are practically the same for angles of incidence above ~40°. However, significant differences in magnitude (e.g., ~10° in Δ) are observed for the higher orders between on- and off-blaze measurements. ϕ_1, $\Delta_{1,2}$, and $\psi_{1,2}$ are in degrees.

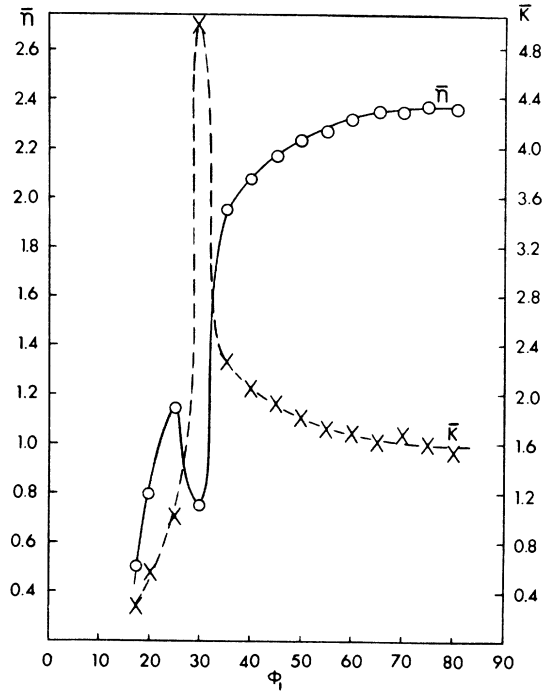

FIG. 4. Pseudo-refractive-index $\bar{n}$ and extinction coefficient $\bar{k}$ of an equivalent (perfectly smooth) substrate that would result in the same polarization behavior of the specular beam as does the grating surface. This is computed from Eq. (7) at each angle of incidence ϕ_1 with ρ_0 determined by ψ_0 and Δ_0 of Fig. 2. ϕ_1 is in degrees.

become increasingly more p polarized as ϕ_1 approaches grazing incidence. Note that the degree of p polarization also increases with the order of the diffracted beam.

IV. EXPLANATION OF POLARIZATION OF SPECULARLY REFLECTED ORDER AND ASSESSMENT OF OPTICAL EFFECT OF SURFACE ROUGHNESS

Analysis of the information contained in the polarization behavior of the radiation specularly reflected from a grating surface will be related to the more general problem of surface roughness. The grating simply offers an example of a periodic rough surface.

If h denotes the depth of the triangular groove of the echelette grating, the maximum deviation from the MSL, σ_{max}, and the rms roughness, σ_{rms} (obtained from the periodic saw-tooth profile using the definition of the rms value), will be

$$\sigma_{max} = \tfrac{1}{2}h\,, \quad \sigma_{rms} = h/2\sqrt{3}\,. \tag{6}$$

For interline spacing of 8333.3 Å and groove angles of 10.3° and 60°, one finds that $h = 1362$ Å, $\sigma_{max} = 681$ Å, and $\sigma_{rms} = 393$ Å. The above surface is moderately rough because $\sigma_{rms}/\lambda = 0.16$. Using a simple argument, it can be shown that the surface appears less and less rough as ϕ_1 (the angle of incidence) is increased. An effective rms roughness, defined as $\sigma_{rms}\cos\phi_1$, goes to zero at large angles of incidence.

It is interesting to calculate the complex pseudo-refractive-index $\bar{N}$ of an equivalent perfectly smooth substrate which would result in the same polarization characteristic for the specular beam as does the grating surface. Using the experimental value of $\rho_0 \equiv \tan\psi_0 e^{i\Delta_0}$, $\bar{N}$ is given by[15]

$$\bar{N} = N_S \sin\phi_1\left[1+\left(\frac{1-\rho_0}{1+\rho_0}\right)^2 \tan^2\phi_1\right]^{1/2}, \tag{7}$$

where N_S is the refractive index of the surrounding medium, in this case air, and can be taken as unity at the wavelength of measurement. From Eq. (7) and (ψ_0, Δ_0) of Fig. 2, we obtained $\bar{n}$ and $\bar{k}$ of Fig. 4, where $\bar{n} - i\bar{k} = \bar{N}$. The marked variation of the pseudoconstants in the vicinity of $\phi_1 = 30°$ is not unexpected and reflects the corresponding variation of (ψ_0, Δ_0) in Fig. 2. Of greater importance is the variation of $\bar{n}$ and $\bar{k}$ with ϕ_1 at large angles of incidence, namely, from $\phi_1 \approx 45°$ to $\phi_1 = 80°$. Over this range the pseudo-refractive-index $\bar{n}$ decreases monotonically from 1.157 to 0.961, a drop of about 20%. Meanwhile, the pseudo-extinction-coefficient $\bar{k}$ increases monotonically from 3.958 to 4.290, a rise of about 8%. Such variations in the pseudoconstants suggest that the grating surface be represented by a filmed substrate which is known to behave in a similar way. The film thickness obtained from using this model is expected to be in a range intermediate between very thin and relatively thick films. This follows because the pseudoconstants of filmed substrates obtained using very small film thickness ($\sim \frac{1}{100}\lambda$) show hardly any change with angle of incidence, whereas large thicknesses ($\sim \frac{1}{2}\lambda$) lead to large oscillatory variations characteristic of interference resonances within the film. In the following we will search for the optical parameters of a reflecting structure composed of a perfectly smooth substrate with a uniform overlay film that would reproduce the variation of (ψ_0, Δ_0) with ϕ_1 actually obtained for the grating. The optical parameters include the complex refractive indices of the substrate and the film as well as the film thickness. At first the film will be assumed homogeneous throughout its thickness. Subsequently we will discuss the inhomogeneous-film model.

A. Homogeneous-Film Model

The values of ψ_i and Δ_i which determine the change in the state of polarization of light of wavelength λ upon reflection at an angle ϕ_i from a filmed substrate are given by

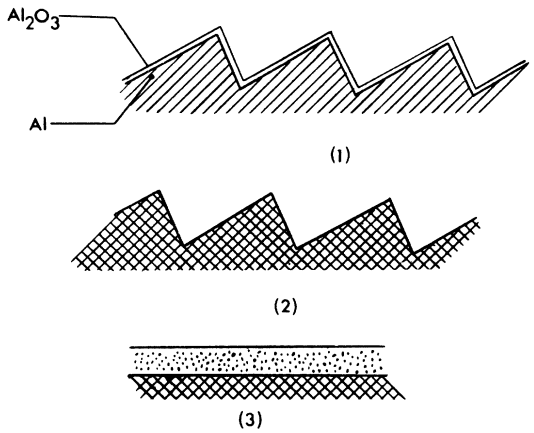

FIG. 5. Optical model used to explain the polarization characteristic of the specularly reflected zeroth-order beam. First the effect of the natural-oxide layer is absorbed by using an effective index of refraction to characterize the oxidized aluminum surface, (1) → (2). Next the roughened portion of the surface is represented by a uniform film on top of a smooth substrate whose optical properties are those of oxidized aluminum, (2) → (3).

$$\psi_i = \psi(N_B,\ N_F,\ t_F,\ \lambda,\ \phi_i)\ ,$$
$$\Delta_i = \Delta(N_B,\ N_F,\ t_F,\ \lambda,\ \phi_i)\ , \tag{8}$$

where N_B and N_F are the complex refractive indices of the substrate and the film and t_F is the film thickness. The explicit functional form of Eq. (8) is given by the exact Drude equations.[15] A computer program developed in this laboratory[16,17] was used to obtain a solution for the parameters N_B, N_F, and t_F by minimizing the sum of squares

$$S = \sum_{i=1} [(\psi - \psi_0)_i^2 + (\Delta - \Delta_0)_i^2]\ , \tag{9}$$

where $(\psi_0,\ \Delta_0)_i$ denote the measured ellipsometric angles for the zeroth-order beam at the ith angle of incidence ϕ_i and $(\psi,\ \Delta)_i$ refer to values computed for a filmed substrate using Eq. (8). From data at seven angles of incidence ($50° \leq \phi \leq 80°$ in steps of 5° each) and with N_B, N_F, and t_F all allowed to vary, the values that provide a least-squares fit were found to be

$$N_B = 0.493 - i\,4.061\ ,$$
$$N_F = 4.29 - i\,0.085\ , \tag{10}$$
$$t_F = 745.9\ \text{Å}\ .$$

The values of ψ and Δ computed using the parameters of Eq. (10) are indicated on Fig. 2 by the open triangles and circles, respectively.

The optical parameters in Eq. (10) can be explained on the basis of the model in Fig. 5. First the effect of the natural oxide(Al_2O_3) is taken care of by using a modified index of refraction to characterize the oxidized aluminum surface. Next the effect of the roughened portion of the surface is represented by a uniform film on top of a smooth substrate whose index of refraction is that of oxidized aluminum. Indeed, the value of N_B in Eq. (10) corresponds reasonably to the optical constants of an $Al + Al_2O_3$ surface. However, if the optical constants of Al are taken to be those measured by Shulz,[18,19] namely, $N(Al) = 1.15 - i\,6.25$, an oxide layer of thickness ~ 135 Å and refractive index ~ 1.65 has to be assumed to give the pseudo-index N_B of Eq. (10). This value of oxide thickness is larger than that generally reported[20,22] for the natural oxide (~ 50 Å). However, there is a spread in the values of the optical constants of freshly evaporated aluminum reported in the literature, depending on evaporation conditions.[18–22] For example, the oxide thickness could be reduced to one-half the above value if an index of refraction of $0.75 - i\,5.15$ is assigned to the aluminum. This value is not unrealistic and can be due to poor vacuum conditions.

The film thickness of Eq. (10) is comparable with one-half the depth of the triangular grooves. To explain the film index of Eq. (10) we averaged the indices of air and oxidized Al according to the Maxwell Garnett theory.[23] At large angles of incidence, the light senses the roughened surface as though it were smoothed out and has an apparent refractive index between that of air and oxidized Al. If the volume fraction of the substrate material with index N_B in the roughened layer is denoted by q, the effective index of refraction N_e is given by

$$N_e^2 = (1 + 2rq)/(1 - rq)\ ,$$
$$r = (N_B^2 - 1)/(N_B^2 + 2)\ . \tag{11}$$

Assuming $q = \frac{1}{2}$ (since the groove is triangular) and using N_B of Eq. (10), an effective index of $2.33 - i\,0.108$ is obtained. Although the extinction coefficient agrees quite well with that of the film in Eq. (10), the refractive index is lower. In spite of this discrepancy, these results, which were obtained from analyzing the polarization characteristics of the zeroth-order specularly reflected beam of a grating surface, represent an important step in understanding the effect of surface roughness. Although the idea of representing a rough surface by a filmed substrate was proposed earlier by Fenstermaker and McCrackin,[24] heretofore there has been no experimental confirmation of its validity.

B. Inhomogeneous-Film Model

This is obtained by assuming a local filling factor q that varies linearly from 1 to 0 over a dis-

tance of h (the groove depth). In this model the film thickness is equal to h and the law of variation of film index with depth into the film is determined by Eq. (11). The only variable parameter is N_B. By trying various values of N_B, a good fit between values of ψ and Δ calculated from the inhomogeneous-film model and those actually measured for the zeroth-order beam was obtained at $N_B = 0.542 - i4.355$. This value of the refractive index is somewhat higher than the value obtained for the substrate in the homogeneous-film case and corresponds to an oxidized aluminum surface where $N(\mathrm{Al}) = 0.75 - i5.15$, $N(\mathrm{Al_2O_3}) = 1.65$, and there is oxide thickness of 52.5 Å.

Two points need to be made regarding the calculations of the inhomogeneous-film case. One is that the inhomogeneous film was replaced by strata of subfilms each with an index corresponding to the local filling factor q. With groove depth $h = 1362$ Å it was found that the number of films has to be increased to as high as 4000 to reach saturation of the computed ψ and Δ. This number corresponds to subfilm thickness of a small fraction of an angstrom. The computed values of ψ and Δ are extremely sensitive to N_B but insensitive to uncertainties in h as large as 5%. The second point pertains to the equivalence between an inhomogeneous film and a homogeneous one with properly defined thickness and index of refraction. The above results indicate that such equivalence is possible and lead to the conclusion that ellipsometry alone cannot resolve the film-index profile. However, the exact relations between the parameters of the equivalent homogeneous film and the law of variation and thickness of the inhomogeneous film do not exist. The expression given by McCrackin and Colson[25] for the thickness of the equivalent film does not apply when the film is absorbing, because it can lead to a complex thickness, and the one for the equivalent index has been found to yield completely erroneous results in this case.

In conclusion, from ellipsometric measurements on the zeroth-order diffracted beam from a grating we have shown that the optical effect of surface roughness can be accounted for by replacing the roughened layer by a film whose index is obtained by the Maxwell Garnett theory as the average of the indices of the material of the surface and that of the immersion medium and whose thickness gives a measure of the degree of surface roughness. These results are particularly applicable when the surface is not excessively rough and at large angles of incidence.

V. COMPARISON WITH PREDICTIONS OF PHYSICAL-OPTICS APPROXIMATION

An exact expression for the electric vector of the radiation field at a point P far removed from the surface S of a grating illuminated by an incident plane wave is given by the Stratton-Silver-Chu integral[26]

$$\vec{\mathrm{E}}(P) = A\hat{k}_2 \times \int\int_S [\hat{n}\times\vec{\mathrm{E}} - \eta\hat{k}_2\times(\hat{n}\times\vec{\mathrm{H}})] \times e^{ik(\hat{k}_2-\hat{k}_1)\cdot\vec{r}}\,dS\,, \quad (12)$$

where $\hat{k}_1$ and $\hat{k}_2$ are unit vectors in the direction of propagation of the incident and scattered waves, respectively; $\vec{\mathrm{E}}$ and $\vec{\mathrm{H}}$ are the electric and magnetic field vectors at the point $\vec{r}$ on the surface where the local normal is $\hat{n}$. Finally,

$$k = 2\pi/\lambda, \quad \eta = (\mu/\epsilon)^{1/2}, \qquad A = ike^{ikR_0}/4\pi R_0\,, \quad (13)$$

where μ and ϵ are the permeability and permittivity of the immersion medium and R_0 is the distance from the origin to the field point P.

The physical-optics approximation[27,28] assumes that the $\vec{\mathrm{E}}$ and $\vec{\mathrm{H}}$ fields at any point on the surface S are the same as they would be if that point were part of an infinite tangent plane. Therefore the Fresnel reflection formulas are assumed to hold locally at each point with the angle of incidence taken to be that between the incident wave vector and the local normal. Besides, the local dielectric constant can be used if the surface is inhomogeneous.

When the wave vector of the incident light is perpendicular to the grooves of the grating, the geometry of the problem simplifies considerably. Because of symmetry, the scattered radiation is confined to the plane of incidence, i.e., the yz plane in Fig. 6. Let $(\hat{s}, \hat{t}, \hat{n})$ be a right-handed mutually orthogonal set of unit vectors defined at each point on the surface of the grating, where $\hat{s}$ and $\hat{t}$ represent the local unit tangents parallel to the rulings (i.e., along the x direction) and tangent to the groove profile, respectively, and $\hat{n} = \hat{s}\times\hat{t}$ is the local unit normal as before. Now we consider separately the two cases of p and s polarization in which the electric vector of the incident wave is either polarized parallel (p) or perpendicular (s) to the plane of incidence. After simple vector-algebraic manipulations the quantities in the integrand of Eq. (12) involving the field vectors become

$$\hat{n}\times\vec{\mathrm{E}} = E_{ip}(R_p - 1)\cos\theta\,\hat{s}\,, \qquad \eta\hat{n}\times\vec{\mathrm{H}} = E_{ip}(R_p + 1)\hat{t} \quad (14)$$

for the case of p polarization and

$$\hat{n}\times\vec{\mathrm{E}} = E_{is}(R_s + 1)\hat{t}\,, \qquad \eta\hat{n}\times\vec{\mathrm{H}} = -E_{is}(R_s - 1)\cos\theta\,\hat{s} \quad (15)$$

for s polarization, where E_{ip} and E_{is} are the complex-field amplitudes of the incident wave of the

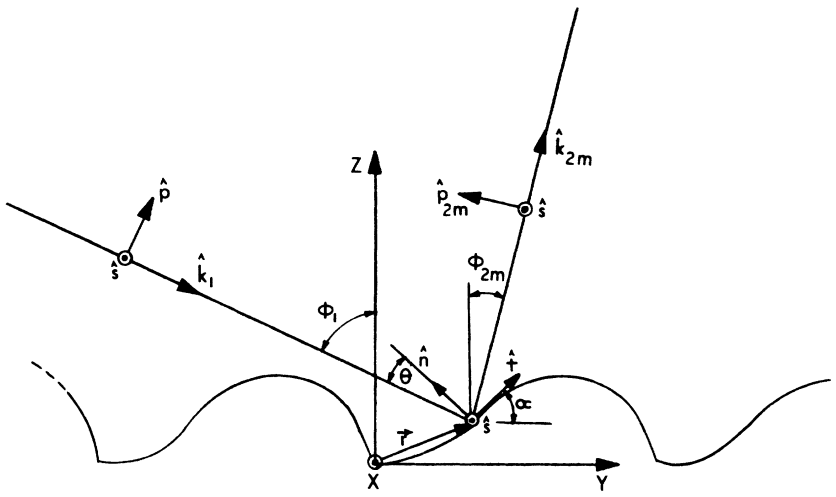

FIG. 6. Definition of the various directions and angles mentioned in Sec. V. (x, y, z) is a right-handed Cartesian coordinate system with x running parallel to the grooves and z normal to the mean surface level (MSL). $(\hat{s}, \hat{t}, \hat{n})$ is a right-handed mutually orthogonal set of unit vectors defined at each point with position vector $\vec{r}$ on the surface of the grating where $\hat{s}$ and $\hat{t}$ are parallel to the rulings and tangent to the groove profile, respectively, and $\hat{n} = \hat{s} \times \hat{t}$ is the local unit normal. $\hat{k}_1$ and $\hat{k}_{2m}$ are unit vectors in the direction of propagation of the incident and mth diffracted waves, respectively. ϕ_1 and ϕ_{2m} are the angle of incidence and the angle of diffraction of the mth order, respectively, and θ is the local angle of incidence. The directions of polarization $\hat{s}$, $\hat{p}$, and $\hat{p}_{2m}$ follow the usual conventions.

respective polarizations and R_p and R_s are the local Fresnel reflection coefficients, which are functions of local angle of incidence θ.

Because the radiation scattered by the grating surface is known to be beamed along the directions predicted by the grating equation (5), we will be interested only in the far fields along these diffracted orders. Let $\hat{k}_{2m}$ be the unit vector in the direction of propagation of the mth radiating space harmonic (i.e., the mth diffracted order). The radiation field at a point far removed from the grating surface along this direction is obtained by substituting from Eqs. (14) and (15) into Eq. (12). Carrying out the various vector multiplications involved, we get the radiation fields of the mth order for both polarizations:

$$\vec{E}^m_{rp} = -\hat{p}_{2m} A E_{ip} \int\int_S [(R_p - 1)\cos(\phi_1 - \alpha) + (R_p + 1)\cos(\phi_{2m} + \alpha)] \exp[ik(\hat{k}_{2m} - \hat{k}_1)\cdot\vec{r}]\, dS \ , \tag{16}$$

$$\vec{E}^m_{rs} = -\hat{s} A E_{is} \int\int_S [(R_s - 1)\cos(\phi_1 - \alpha) + (R_s + 1)\cos(\phi_{2m} + \alpha)] \exp[ik(\hat{k}_{2m} - \hat{k}_1)\cdot\vec{r}]\, dS \ , \tag{17}$$

where α is the local angle of inclination of the groove side measured from the MSL (i.e., the angle between $\hat{t}$ and the y direction), $\hat{p}_{2m} = -\hat{k}_{2m} \times \hat{s}$, and ϕ_1 and ϕ_{2m} are the angles of incidence and diffraction of the mth order as before. Dividing Eq. (16) by Eq. (17) and making use of the definition of ρ_m in Eq. (3), we find

$$\rho_m = \frac{\int [(R_p + 1)\cos(\phi_{2m} + \alpha) + (R_p - 1)\cos(\phi_1 - \alpha)] \exp[ik(\hat{k}_{2m} - \hat{k}_1)\cdot\vec{r}]\, dS}{\int [(R_s + 1)\cos(\phi_{2m} + \alpha) + (R_s - 1)\cos(\phi_1 - \alpha)] \exp[ik(\hat{k}_{2m} - \hat{k}_1)\cdot\vec{r}]\, dS} \ , \tag{18}$$

which is the ellipsometrically measured quantity. Equation (18) represents the main result obtained using the physical-optics approximation. The dependence on the detailed groove shape is contained both explicitly in α and $\vec{r}$ and implicitly in R_p and R_s. The latter are functions of the local angle of incidence $\theta = \phi_1 - \alpha$ and the complex dielectric constants of the materials forming the grating surface. Since there is no variation in the x direction, dS in Eq. (18) signifies the element of arc of the cross section (profile) of the grating, and a single integral therefore replaces the double integral. Because of the periodicity in the y direction an array factor could be dropped from both the numerator and denominator of Eq. (18) and the integrals can be taken over one period only.

For an echelette grating with groove sides of lengths a and b inclined at angles α and β, respectively, from the MSL, the integration in Eq. (18) can be carried out to give the closed-form solution

$$\rho_m = (A_p + B)/(A_s + B) \ , \tag{19}$$

where

$$A_{p,s} = R_{p,s}(\phi_1 - \alpha)\frac{F_1}{H_1}\left(e^{i(2\pi a/\lambda)H_1} - 1\right)$$

$$-R_{p,s}(\phi_1+\beta)\frac{F_2}{H_2}\,(e^{-i(2\pi b/\lambda)H_2}-1)\ ,$$

$$B=\frac{G_1}{H_1}\,(e^{i(2\pi a/\lambda)H_1}-1)-\frac{G_2}{H_2}\,(e^{-i(2\pi b/\lambda)H_2}-1)\ , \qquad (20)$$

$$\begin{aligned}
F_1&=\cos(\phi_{2m}+\alpha)+\cos(\phi_1-\alpha)\ ,\\
F_2&=\cos(\phi_{2m}-\beta)+\cos(\phi_1+\beta)\ ,\\
G_1&=\cos(\phi_{2m}+\alpha)-\cos(\phi_1-\alpha)\ ,\\
G_2&=\cos(\phi_{2m}-\beta)-\cos(\phi_1+\beta)\ ,\\
H_1&=\sin(\phi_{2m}+\alpha)-\sin(\phi_1-\alpha)\ ,\\
H_2&=\sin(\phi_{2m}-\beta)-\sin(\phi_1+\beta)\ .
\end{aligned} \qquad (21)$$

$R_{p,s}$ are the Fresnel coefficients

$$\begin{aligned}
R_p(\theta)&=\frac{\epsilon'\cos\theta-(\epsilon'-\sin^2\theta)^{1/2}}{\epsilon'\cos\theta+(\epsilon'-\sin^2\theta)^{1/2}}\ ,\\
R_s(\theta)&=\frac{\cos\theta-(\epsilon'-\sin^2\theta)^{1/2}}{\cos\theta+(\epsilon'-\sin^2\theta)^{1/2}}
\end{aligned} \qquad (22)$$

for reflection at angle of incidence θ from a surface with an effective dielectric constant ϵ'. The results in Eqs. (19)–(22) complete the solution of the problem within the limits of the physical-optics approximation.

Now we return to Fig. 2, which gives the change of the ellipsometric angles ψ_0 and Δ_0 of the zeroth-order beam with angle of incidence. The pronounced variation around $\phi_1=30°$ coincides with the onset of the shadowing of one side of the triangular groove as the angle of incidence exceeds $\phi_1=\frac{1}{2}\pi-\beta$, where $\beta=60°$. Using the index of refraction of Eq. (10) to characterize the oxidized Al surface of the grating, the results of the physical-optics approximation were obtained using Eqs. (19)–(22). Shadowing was accounted for by assuming zero fields on one side of the groove when $\phi_1>\frac{1}{2}\pi-\beta$. The results are shown in Fig. 7. Note that, whereas the variation in Δ_0 around $\phi_1=30°$ can be reasonably reproduced, only a change of slope in the ψ_0 curve is obtained at this angle. At large angles of incidence the general behavior is the same, though the theoretical values are far below those obtained from experiment. Better agreement can be expected if nonzero values for the fields are assumed at points on the groove surface in the geometrical shadow. For example, the theoretical results of the diffraction by the edge of an infinite half-plane can be used. The above results indicate the need for a complete solution of the boundary-value problem for *both* of the p and s polarizations taking due account of the effect of *finite* conductivity at optical frequencies.

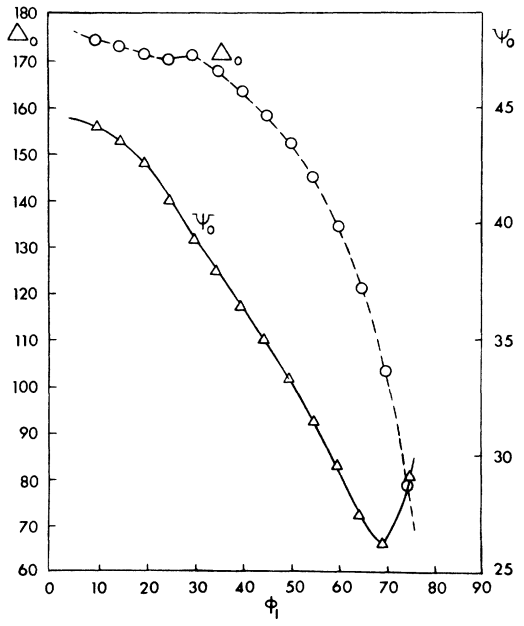

FIG. 7. Values of ψ_0 and Δ_0 of the zeroth-order beam computed from Eqs. (19)–(22) using the physical-optics approximation. This figure should be compared with the experimental results of Fig. 2. ϕ_1, Δ_0, and ψ_0 are in degrees.

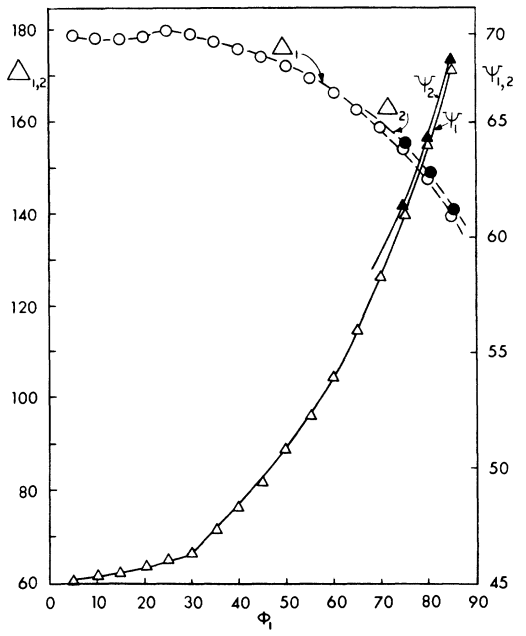

FIG. 8. Same as in Fig. 7 for the first and second diffracted orders. The results in this case are to be compared with those of Fig. 3. ϕ_1, $\Delta_{1,2}$, and $\psi_{1,2}$ are in degrees.

The results for the first and second orders are shown in Fig. 8. The dependence of (ψ_1, Δ_1) and (ψ_2, Δ_2) on ϕ_1 is predicted qualitatively by the physical-optics approximation. However, there is an appreciable difference in magnitudes. Again the need for a complete theoretical treatment cannot

be overemphasized.

VI. CONCLUSIONS

Ellipsometry provides a useful technique in the study of the polarization characteristics of the radiation scattered from the surface of a diffraction grating. The ratio ρ_m of the far-field complex reflection coefficients for the p and s polarizations can be measured for any diffracted order m. The set of complex numbers ρ_m ($m = 0, \pm 1, \pm 2, \ldots$) specifies the elliptic polarization forms of the various diffracted orders for any given state of polarization of the incident beam. This information is complementary to that which pertains to the division of the scattered energy over the various orders of diffraction.

Results are reported for measurements made on an aluminum-coated 1200-lines/mm echelette diffraction grating. The polarization properties of the zeroth-, first-, and second-order beams are studied at $\lambda = 6328$ Å over a range of angle of incidence 17.5°–80°. We have shown that the optical effect of surface roughness can be accounted for by replacing the roughened layer by a film whose index of refraction is obtained from the theory of Maxwell Garnett as the average of the indices of the material of the surface and that of the immersion medium and whose thickness is a measure of the degree of surface roughness.

An exact solution of the problem of the scattering of light of p and s polarizations by a diffraction grating which accounts for the effect of finite conductivity has not yet been developed. For this reason we have compared our results with those predicted by the physical-optics approximation. A closed-form solution for ρ_m has been derived starting from the Stratton-Silver-Chu integral. There is agreement between the gross features of both the theory and the experiment. However, exact magnitudes could not be compared. This points to the need for more effort to completely solve the grating boundary-value problem.

---

*Work supported by the National Science Foundation.
†Supported in part by the U. S. Office of Naval Research.

[1]G. W. Stroke, in *Handbuch der Physik*, edited by S. Flügge (Springer-Verlag, Berlin, 1967), Vol. XXIX, p. 426.
[2]E. Brannen, Proc. IEEE 53, 2134 (1965).
[3]W. Q. Jeffers, Appl. Phys. Letters 11, 178 (1967).
[4]H. P. Bonzel and N. A. Gjostein, Appl. Phys. Letters 10, 258 (1967); J. Appl. Phys. 39, 3480 (1968).
[5]J. J. Cowan and E. T. Arakawa, Z. Physik 235, 97 (1970), and references therein.
[6]R. Petit, Rev. Opt. 45, 249 (1966).
[7]T. Itoh and R. Mittra, IEEE Trans. Microwave Theory Tech. 17, 319 (1969).
[8]A. R. Neureuther and K. Zaki, Alta Frequenza 38, 283 (1969).
[9]R. B. Green, IEEE Trans. Microwave Theory Tech. 18, 313 (1970).
[10]H. A. Kalhor and A. R. Neureuther, J. Opt. Soc. Am. 61, 43 (1971).
[11]K. A. Zaki and A. R. Neureuther, IEEE Trans. Antennas Propagation 19, 208 (1971).
[12]R. M. A. Azzam and N. M. Bashara, J. Opt. Soc. Am. 62, 222 (1972); 62, 336 (1972); Opt. Commun. 4, 203 (1971).
[13]R. M. A. Azzam and N. M. Bashara, J. Opt. Soc. Am. 61, 600 (1971); 61, 773 (1971); 61, 1118 (1971); 61, 1236 (1971); 61, 1380 (1971).
[14]Values provided by the manufacturer. An uncertainty of 10° in β around 60° does not appreciably affect the conclusions of Sec. V. The value $\beta = 60°$ was found to provide the best fit between theory and experiment.
[15]A. Vašíček, *Optics of Thin Films* (North-Holland, Amsterdam, 1960).
[16]J. A. Johnson, Ph.D. dissertation (University of Nebraska, 1970) (unpublished).
[17]J. A. Johnson and N. M. Bashara, J. Opt. Soc. Am. 61, 457 (1971).
[18]L. G. Shulz, J. Opt. Soc. Am. 44, 357 (1954).
[19]L. G. Shulz and F. R. Tangherlini, J. Opt. Soc. Am. 44, 362 (1954).
[20]P. H. Berning, G. Hass, and R. P. Madden, J. Opt. Soc. Am. 50, 586 (1960).
[21]G. Hass and J. E. Waylonis, J. Opt. Soc. Am. 51, 719 (1961).
[22]R. W. Fane and W. E. Neal, J. Opt. Soc. Am. 60, 790 (1970).
[23]O. S. Heavens, *Optical Properties of Thin Solid Films* (Butterworths, London, 1955), p. 177.
[24]C. A. Fenstermaker and F. L. McCrackin, Surface Sci. 16, 85 (1969); also in *Proceedings of the Symposium on Recent Developments in Ellipsometry*, edited by N. M. Bashara, A. B. Buckman, and A. C. Hall (North-Holland, Amsterdam, 1969).
[25]F. L. McCrackin and J. P. Colson, in *Ellipsometry in the Measurement of Surfaces and Thin Films*, edited by E. Passaglia, R. R. Stromberg, and J. Kruger, Natl. Bur. Std. Misc. Publ. No. 256 (U.S. GPO, Washington, D. C., 1964), p. 61.
[26]S. Silver, *Microwave Antenna Theory and Design* (McGraw-Hill, New York, 1947), p. 161.
[27]P. Beckman, *The Depolarization of Electromagnetic Waves* (Golem, Boulder, Colo., 1968), p. 76.
[28]A. K. Fung, Proc. IEEE 54, 395 (1966).